

ORIGINAL ARTICLE

Blockade of inhibitors of apoptosis (IAPs) in combination with tumor-targeted delivery of tumor necrosis factor- α leads to synergistic antitumor activityZ Yuan¹, G Syrkin¹, A Adem¹, R Geha¹, J Pastoriza¹, C Vrikshajani¹, T Smith², TJ Quinn¹, G Alemu¹, H Cho¹, CJ Barrett¹, W Arap², R Pasqualini² and SK Libutti¹

In the current study, we examined whether the combination of tumor vasculature-targeted gene therapy with adeno-associated virus bacteriophage-tumor necrosis factor- α (AAVP-TNF- α) and/or the orally administered LCL161, an antagonist of inhibitors of apoptosis proteins (IAPs), enhanced antitumor efficacy without systemic toxicity. M21 human melanoma xenografts were grown subcutaneously in nude mice. Mice were treated according to one of four treatment regimens: AAVP-TNF- α alone (AAVP-TNF- α plus sodium acetate-acetic acid (NaAc) buffer) via tail vein injection; LCL161 alone (phosphate-buffered saline (PBS) plus LCL161) via oral gavage; AAVP-TNF- α plus LCL161; and PBS plus NaAc Buffer as a control group. Tumor volume, survival and toxicity were analyzed. AAVP trafficking and TNF- α production *in vivo* were detected on days 7 and 21 by real-time PCR, enzyme-linked immunosorbent assay and immunofluorescence. The levels of apoptosis and activation of caspases were assessed on days 7 and 21 by TUNEL (terminal deoxynucleotidyltransferase-mediated dUTP nick end labeling) and immunofluorescence assays. Our results showed that the combination of AAVP-TNF- α and LCL161 significantly inhibited tumor growth and prolonged survival in mice with melanoma xenografts. The combination of AAVP-TNF- α and LCL161 was also significantly more effective than either agent alone, showing a synergistic effect without systemic toxicity.

Cancer Gene Therapy (2013) **20**, 46–56; doi:10.1038/cgt.2012.83; published online 16 November 2012

Keywords: targeted gene therapy; conventional chemotherapy; adeno-associated virus bacteriophage-tumor necrosis factor- α (AAVP-TNF- α); LCL161; apoptosis

INTRODUCTION

Systemically delivered therapies often have significant unwanted side effects because of their indiscriminant activity on both neoplastic and normal tissue. Targeted therapy, whether for a specific tissue type or pathway, is indicated as a strategy for cancer treatment because it theoretically delivers the anticancer agent directly to the site of the tumor. Recently, we have been developing hybrid bacteriophages (phage) based on prokaryotic viruses that represent a promising vector strategy for the delivery of therapeutic transgenes.^{1–3} Systemic administration of bacteriophages has been shown to be an effective therapy for antibiotic-resistant septicemia in patients,⁴ and can be safely used in immunocompromised patients without significant toxicity.⁵

Tumor necrosis factor- α (TNF- α) is a cytokine that affects tumor cells and the tumor microenvironment. Several clinical trials have been performed to investigate the efficacy of TNF- α in treating patients with cancer.^{6–13} However, systemic administration of TNF- α as an anticancer agent at therapeutic doses is limited by the severe systemic side effects, such as hypotension and organ failure.¹⁴ To avoid the side effects caused by the systemic administration of TNF- α , we previously developed a novel vector, RGD-AAVP-TNF- α ,^{6,15} to target TNF- α directly to the tumor. This system incorporates an adeno-associated virus bacteriophage (AAVP) vector engineered to selectively target tumor-associated

vasculature by expression of an RGD (arginine-glycine-aspartic acid) amino-acid motif (termed RGD-4C) on its surface.^{16–18} This motif binds to the ligand $\alpha v \beta 3$, an integrin often found to be overexpressed on tumor vascular endothelium.^{16–18} Thus, RGD-AAVP-TNF- α can be administered systemically but delivers its gene product specifically to the tumor vasculature, thereby avoiding systemic toxicity. After intravenous administration in animal models, RGD-AAVP-TNF- α was found in tumor-associated blood vessels, but not in healthy tissues. Furthermore, sustained expression of TNF- α was detected only in tumor tissue; the exposure of normal tissue beds during a therapeutic response was therefore minimized.^{19,20} Although this previous work demonstrated selected targeting of TNF- α using RGD-AAVP vector, there was only a relatively modest effect on tumor growth and survival.^{19,20} An important aspect of TNF- α activity is its induction of apoptosis in both tumor and endothelial cells. We therefore questioned whether the TNF- α response we observed could be augmented by agents that enhance apoptosis. Our strategy was to combine targeted expression of TNF- α with other proteins that could enhance these pro-apoptotic effects.

The inhibitor of apoptosis proteins (IAPs) are a family of proteins that inhibit caspases and thereby regulate apoptosis.^{21,22} Smac (second mitochondria-derived activator of caspases) is a pro-apoptosis mitochondrial protein that is released into the cytosol

¹Department of Surgery, Albert Einstein College of Medicine, Bronx, NY, USA and ²Department of Experimental Diagnostic Imaging, The University of Texas MD Anderson Cancer Center, Houston, TX, USA. Correspondence: Professor SK Libutti, Montefiore-Einstein Center for Cancer Care, Albert Einstein College of Medicine, Greene Medical Arts Pavilion 4th Floor, 3400 Bainbridge Avenue, Bronx, NY10467, USA.

E-mail: slibutti@montefiore.org

Received 22 May 2012; revised 28 September 2012; accepted 4 October 2012; published online 16 November 2012

upon an apoptotic stimuli and binds to the IAPs.^{23,24} Smac and Smac mimetics can induce proteasomal degradation of cellular IAPs (cIAPs), resulting in increased apoptosis.^{23,24} LCL161 is an orally bioavailable mimetic of Smac that binds to and mediates the degradation of several IAPs (XIAP, cIAP1 and cIAP2) and induces apoptosis via caspase activation.²⁵ The high-affinity binding of LCL161 to IAPs and their subsequent destruction results in the activation of noncanonical nuclear factor- κ B signaling, and a subsequent increase in TNF- α production and autocrine stimulation of TNF receptor 1 and further induction of caspase 9.^{26–30} Recently, XIAP, cIAP1 and cIAP2 were reported to be elevated in many cancers, with subsequent resistance to the induction of apoptosis by TNF- α .^{31,32} We therefore hypothesized that the combination of this Smac mimetic, LCL161, with our tumor-targeted TNF- α biotherapeutic agent would lead to enhanced apoptosis in tumor cells and tumor-associated vasculature, along with reduced toxicity and the delay or prevention of the development of resistance in a mouse xenograft model of human melanoma. We also examined the effects of this combination on cellular apoptosis and proliferation.

MATERIALS AND METHODS

Cell culture

The M21 human melanoma cell line was purchased from American Type Culture Collection (ATCC, Manassas, VA, USA) and grown at 37 °C as a monolayer culture with RPMI-1640 medium containing 10% fetal bovine serum, 100 U ml⁻¹ penicillin G and 100 μ g ml⁻¹ streptomycin.¹⁷

M21 xenograft mouse experiments

All animal experiments were conducted according to protocols approved by the Animal Institute of Albert Einstein College of Medicine (Bronx, NY, USA). Female, 6-week-old nude mice were purchased from Jackson Laboratories (Bar Harbor, ME, USA). M21 human melanoma cells (4×10^6) were implanted subcutaneously into the right flank. At 2 weeks after implantation, tumor volumes (mm³) were measured in three dimensions and were calculated as length \times width \times height \times 0.52. When tumor volumes reached ~ 100 – 150 mm³, the mice were assigned to groups such that the average tumor size was equivalent in each group.

Treatment of M21 xenografts with AAVP-TNF- α and LCL161

RGD-AAVP-TNF- α was constructed, purified and quantified as described in our published protocols.^{19,20} LCL161 was provided as part of a collaboration with NOVARTIS Pharmaceutical Corporation (Boston, MA, USA). At 2 weeks after tumor cell implantation, mice were treated according to two protocols.

The first protocol evaluated the effects of therapy on the inhibition of tumor growth and on animal survival: 26 M21 xenografted mice were assigned to four groups: (1) Control group ($N=8$) received phosphate-buffered saline (PBS) by tail vein injection weekly (Monday (M)) and received sodium acetate-acetic acid (NaAc) Buffer control by gavage daily (Monday–Friday (M–F)); (2) AAVP-TNF- α group ($N=4$) received AAVP-TNF- α by tail vein injection weekly (M) and was gavaged with NaAc Buffer daily (M–F); (3) LCL161 group ($N=7$) received PBS by tail vein injection weekly (M) and received LCL161 daily (M–F) by gavage; and (4) Combination AAVP-TNF- α plus LCL161 group ($N=7$) received AAVP-TNF- α weekly (M) by tail vein injection and LCL161 daily (M–F) by gavage. All mice were treated for two cycles (Supplementary Table S1 and Supplementary Figure S1). In each cycle, 1×10^{11} AAVP particles (or PBS control) were administered intravenously into the tail vein weekly, and 100 mg kg⁻¹ LCL161 (or NaAc Buffer control) was administered by gavage daily for 4 weeks. In the LCL161 treatment groups, we maintained LCL161 at a dose of 100 mg kg⁻¹ daily (M–F).

The second protocol was designed to examine vector trafficking, gene expression and activation of apoptotic pathways: 24 M21 xenografted mice were assigned to four groups: (1) Control group ($N=6$) received PBS weekly by tail vein injection (M) and NaAc Buffer daily (M–F) for 7 days ($N=3$) or 21 days ($N=3$); (2) AAVP-TNF- α group ($N=6$) received AAVP-TNF- α by tail vein weekly (M) and NaAc Buffer daily (M–F) by gavage for 7 days ($N=3$) or 21 days ($N=3$); (3) LCL161 group ($N=6$) received PBS weekly by tail vein injection (M) and LCL161 daily (M–F) by gavage for

7 days ($N=3$) or 21 days ($N=3$); and (4) Combination AAVP-TNF- α plus LCL161 group ($N=6$) received AAVP-TNF- α weekly (M) by tail vein injection and LCL161 daily (M–F) by gavage for 7 days ($N=3$) or 21 days ($N=3$). Animals were killed at the established time intervals (Supplementary Table S2). Resected tumor tissues and normal tissues (liver, kidney, heart, spleen and skeletal muscle) were flash-frozen and stored at -80 °C. Formalin-fixed tissue was paraffin embedded for further analysis. Peripheral blood was also collected from all animals at days 0, 7 and 21.

Tumor size and survival analysis

We defined tumor growth as an increase in tumor volume, measured in a blinded fashion for average diameter before, during and after treatment. Tumor volume was calculated according to the equation: tumor size = length \times width \times height \times 0.52.^{19,20} The treatment resistance response was analyzed after a total of two cycles. We followed the survival time in each group during and after treatment, and we calculated the average tumor-specific survival rate and tumor-free survival rate for each group.

Toxicity assay

We assessed toxicity in each group *in vivo* by analysis of body mass, feeding status and mobility. All mice were weighed once per week.

Analysis of drug combined effects

Drug synergy was analyzed and quantified by the drug combination-index (CI) methods using CalcuSyn software (Biosoft, Ferguson, MO, USA).³³ The CI method is a mathematical and quantitative representation of a two-drug pharmacologic interaction.³³ We used the drug dose for AAVP-TNF- α and LCL161 from our tumor growth inhibition experiments and, using the CalcuSyn software, we generated CI values over a range of fraction levels (Fa) from 0.05 to 0.90 (5–90% growth inhibition). A CI of 1 indicates an additive effect between AAVP-TNF- α and LCL161, whereas a CI of <1 indicates the presence of synergistic activity.

The *in vivo* AAVP trafficking detection by immunofluorescence assay (IF) with anti-filamentous single-stranded DNA bacteriophage

For detection of AAVP, 5 μ m-thick paraffin sections from the resected tumor tissues and normal tissues (liver, kidney, heart, spleen and skeletal muscle) were stained by dual IF.^{19,20} The sections were incubated overnight at 4 °C in a 1:1000 dilution of rabbit anti-filamentous single-stranded DNA bacteriophage antibody (Sigma Chemical Company, St Louis, MO, USA) and a concentration of 10 ng μ l⁻¹ of antigen affinity-purified rat anti-mouse CD31 antibody (BD Biosciences, San Jose, CA, USA).^{19,20} Slides were next incubated with the secondary antibodies (1:200 dilutions each of goat anti-rabbit Alexa Fluor 647 and goat anti-rat Alexa Fluor 488; Invitrogen, Grand Island, NY, USA) for 45 min in the dark.^{19,20} The slides were mounted in Vectashield mounting medium with 4,6-diamidino-2-phenylindole (DAPI; Vector Laboratories, Burlingame, CA, USA). Images were taken using a fluorescence microscope with camera.

The *in vivo* AAVP-mediated TNF- α transcription detection by real-time PCR

Human TNF- α mRNA was measured by reverse-transcriptase-PCR (RT-PCR) with primer-probe sequences unique to human TNF- α inserted into RGD-AAVP-TNF- α . Total RNA was extracted from frozen tumor and normal tissues (liver, kidney, heart, spleen and skeletal muscle) with RNeasy total RNA kit (Qiagen, Valencia, CA, USA). First-strand complementary DNAs were generated from the total RNA, and quantitative RT-PCR was performed. PCR products were measured as fluorescent signal intensity after standardization with a glyceraldehyde-3-phosphate dehydrogenase (GAPDH) internal control. The following sense and antisense primers and probes for human TNF- α were used: sense primer: 5'-TTCAGCTCTGCATCGTTTTG-3'; antisense primer: 5'-CTCAGCTTGAGGGTTTGCTACA-3', and Probe 5'-FAM-TTCTCTGGCGTCA GATCATCTCTCGAAC-TAMARA-3'.²⁰

The *in vivo* AAVP-mediated TNF- α expression by an enzyme-linked immunosorbent assay (ELISA)

Levels of human TNF- α were assessed by ELISA.^{19,20} Total cell lysates from peripheral blood, frozen tumor tissues and frozen normal tissues (liver, kidney, heart, spleen and skeletal muscle) were prepared in lysis buffer.¹⁹

The amount of protein was quantified using protein assay reagent (Bio-Rad, Hercules, CA, USA). Total protein (100 μ g) was assayed for human TNF- α by ELISA (Biosource, San Francisco, CA, USA).^{19,20}

Measurement of apoptotic cells in tumor tissues by terminal deoxynucleotidyltransferase-mediated dUTP nick end labeling (TUNEL) assay

We assessed the apoptotic status in tumor tissues from control and treated mice at days 7 and 21 by TUNEL assay with an *In Situ* Cell Death Detection Kit (Roche Diagnostic, Indianapolis, IN, USA). The tissue sections were treated with proteinase K (10 μ g ml⁻¹) for 20 min. The sections were next washed twice with PBS, labeled and stained with the TUNEL reaction mixture (label plus enzyme solutions) for 60 min at 37 °C and washed twice with PBS. The slides were mounted in Vectashield mounting medium with DAPI (Vector Laboratories). The apoptotic fluorescent cells were counted under a fluorescent microscope, and the numbers were expressed as the percentage of total cells \pm s.d. A negative control without enzyme treatment and a positive control with DNase I treatment were also performed.

Measurement of the cIAP1 and cIAP2 mRNA expression by real-time RT-PCR

We assessed the mRNA expression levels of cIAP1 and cIAP2 in tumor tissues from control and treated mice groups at days 7 and 21 by real-time RT-PCR. The RT-PCR products were measured as fluorescent signal intensity after standardization with a GAPDH internal control. The following primers for cIAP1 and cIAP2 were used: sense primer for cIAP1: 5'-TGA CTGGCAGG CAGAAATGA-3'; antisense primer for cIAP1: 5'-TTGCCCCGTTGAATCCGAT-3'; sense primer for cIAP2: 5'-TTCAGTAAATGCCGCGAAGAT-3'; antisense primer for cIAP2: 5'-TGGTTTCATGTGCCTGGT-3.

Measurement of the activity of caspase 3 and caspase 9 by IF

We measured the activity of pro-apoptotic pathway components (caspase 3 and caspase 9) in the tumor tissues from control and treated mice at days 7 and 21. The sections were incubated with a concentration of 10 ng μ l⁻¹ of rat anti-mouse CD31 and a concentration of 2.5 ng μ l⁻¹ of rabbit anti-caspase 3 or anti-caspase 9 antibodies (BD Biosciences), respectively, overnight at 4 °C. These antibodies are only able to recognize the active forms of caspase 3 and caspase 9. Sections were further incubated with a 1:200 dilution of anti-rabbit Alexa Fluor 647 and goat anti-rat Alexa Fluor 488 secondary antibodies for 45 min in the dark. The slides were mounted in Vectashield mounting medium with DAPI (Vector Laboratories). Fluorescent cells were counted under a fluorescence microscope, and the numbers were expressed as the percentage of total cells \pm s.d. A negative control without primary antibody was also performed.

Assessment of cell proliferation by IF

We measured cell proliferation in tumor tissues from control and treated mice using proliferating cell nuclear antigen (PCNA). Staining for PCNA on sections was performed in the same manner and used to detect caspase 3 and caspase 9. Rabbit anti-PCNA antibody source (BD Biosciences) was incubated at a concentration of 4 ng μ l⁻¹ overnight at 4 °C. Fluorescent cells were counted under a fluorescence microscope, and the numbers were expressed as the percentage of total cells \pm s.d. A negative control without primary antibody was also performed.

Power calculation and statistical analysis

We used a s.d. of 200 mm and a mean difference between control and treatment groups of 400 mm for tumor volume for the calculation of power based on the two-sided, two-sample student's *t*-test. Using $P < 0.05$, we observed that $n = 3$ mice per group were adequate to achieve a power (1- β) of 90%. The statistical analysis was also conducted to determine significant differences among groups under study, with respect to tumor-specific survival rate, tumor-free survival rate, tumor size, TNF- α expression and apoptotic status and its components. All groups were compared using analyses of variance and Tukey's comparison post-tests (GraphPad Instat software, La Jolla, CA, USA). The *P*-values of < 0.05 were considered statistically significant.

RESULTS

AAVP-TNF- α plus LCL161 enhances the inhibition of tumor growth and delays development of treatment resistance

Tumor volumes in each group were measured and the average diameter was calculated before, during and after treatment. Serial blinded measurements (during and after treatment) of tumor volumes were taken for 120 days (Figure 1 and Supplementary Table S3). The initial tumor volumes (day 0) for all mice from each group were $\sim 115 \pm 24$ mm³. The reduction in tumor volume in the group receiving AAVP-TNF- α plus LCL161 when compared with the other three groups was statistically significant by day 10 after treatment ($P = 0.0001$). The AAVP-TNF- α plus LCL161 treatment group had a mean (\pm s.d.) tumor volume of 235.31 ± 97.00 mm³; the AAVP-TNF- α treatment group had a mean tumor volume of 388.85 ± 188.76 mm³; the LCL161 treatment group had a mean tumor volume of 673.94 ± 118.20 mm³; and the control group had a mean tumor volume of 812.98 ± 324.58 mm³ (Figure 1 and Supplementary Table S3) (day 10). Thus, tumor growth in the AAVP-TNF- α plus LCL161 treatment group was rapidly inhibited in comparison with that of the AAVP-TNF- α -alone treatment group, the LCL161-alone treatment group and control group (Figure 1 and Supplementary Table S3). Antitumor activity was also seen in mice receiving either AAVP-TNF- α alone or LCL161 alone; however, the magnitude of the effect was significantly less than that associated with the combination of the agents (Figure 1 and Supplementary Table S3). In addition, mice in the group receiving combination therapy showed regression of tumors from their baseline measurements and a complete tumor-free response was seen in 3 of the 6 mice (Figure 1). Although the mice receiving either AAVP-TNF- α alone or LCL161 alone exhibited a decrease in the rate of tumor growth, neither group showed evidence of tumor regression (Figure 1).

The development of treatment resistance was analyzed after two cycles of treatment. Tumor growth in the mice receiving the combination of AAVP-TNF- α and LCL161 continued to be inhibited at a $\sim 71\%$ reduction (from 175.96 ± 173.48 mm³ to 51.18 ± 66.05 mm³) in the final tumor volumes in the second cycle (Supplementary Table S3). In contrast, tumor growth in animals receiving AAVP-TNF- α alone was not inhibited (from 1306.42 to 1699.34 mm³) in the second cycle (Supplementary Table S3). There were no live mice in the LCL161-alone treatment group or the control group after the first cycle. Thus, the combination of AAVP-TNF- α plus LCL161 can prevent or delay the development of resistance to treatment, because a repeat cycle again resulted in tumor responses (Figure 1 and Supplementary Table S3).

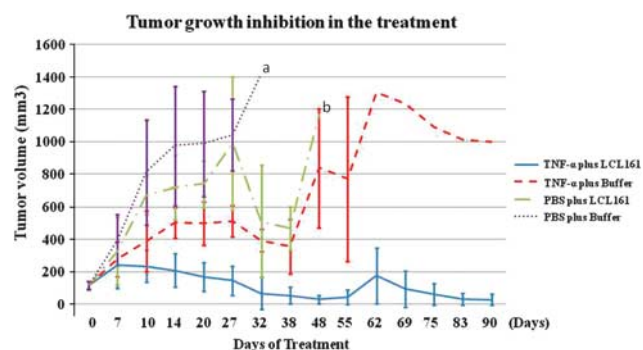


Figure 1. Inhibition of M21 human melanoma xenografts in nude mice treated with targeted adeno-associated virus bacteriophage-tumor necrosis factor- α (AAVP-TNF- α) and/or LCL161. Tumor growth inhibition in all four groups with AAVP-TNF- α plus LCL161; AAVP-TNF- α plus sodium acetate-acetic acid (NaAc) Buffer; phosphate-buffered saline (PBS) plus LCL161; and PBS plus NaAc Buffer treatment from days 0 to 90. ^a: All mice dead in the control group; ^b: all mice dead in the PBS plus LCL161 group.

Treatment with AAVP-TNF- α plus LCL161 prolonged survival in nude mice with human melanoma xenografts

We compared tumor-specific survival and tumor progression-free survival on day 120 in each group. The tumor-specific survival rate was statistically significant among groups ($P < 0.0001$), 100% for the AAVP-TNF- α plus LCL161 treatment group, 25% for the AAVP-TNF- α -alone treatment group, 0% for the LCL161-alone treatment group and 0% for the control group (Figure 2a). One mouse with a small tumor was killed at day 82 in the combination treatment group for a skin infection often seen in nude mice. The necropsy confirmed the cause of death was 'scaly skin' disease and not tumor progression. The median survival time was day 59 for the AAVP-TNF- α -alone treatment group, day 45 for the LCL161-alone treatment group and day 31 for the control group (Figure 2a). The combination group did not reach median survival.

The tumor-free complete response rate on day 120 was 50% for the AAVP-TNF- α plus LCL161 treatment group, and was 0% for the AAVP-TNF- α -alone treatment group, the LCL161-alone treatment group and the control group ($P < 0.0001$; Figure 2b).

Doses of AAVP-TNF- α alone, LCL161 alone and AAVP-TNF- α plus LCL161 did not increase systemic toxicity

We assessed for toxicity in each group by examining their body mass, eating status and mobility. The mice tolerated AAVP-TNF- α and/or LCL161 treatment as demonstrated by no changes in any of these parameters among the four groups (data not shown).

Synergistic effect of AAVP-TNF- α and LCL161 in M21 xenografted nude mice

The additive or potentially synergistic activity of AAVP-TNF- α and LCL161 was evaluated and quantified with CalcuSyn Software, which is a mathematical and quantitative representation of a two-drug pharmacologic interaction.^{33,34} The software generates a CI, where a CI of 1 indicates an additive effect and a CI of < 1 indicates the presence of synergistic activity. We used the drug dose for AAVP-TNF- α and LCL161 from our tumor growth inhibition experiments and generated CI values over a range of fraction levels (Fa) from 0.05 to 0.90 (5–90% growth inhibition). Synergistic activity of AAVP-TNF- α and LCL161 was observed that resulted in combination indices under 0.8 at a fractional effect of 0.5 (50% tumor cell killing) and under 0.5 at a fractional effect of 0.75 (75% tumor cell killing; Figure 3). Thus, AAVP-TNF- α and LCL161 act synergistically, with CI values < 1 as determined with CalcuSyn Software.

AAVP-specific trafficking to tumor vasculature, but not to normal vasculature and normal tissues

The tumor tissues and normal tissues (heart, spleen, kidney, liver and muscle) from each group were removed on days 7 and 21 after treatment. The presence of AAVP particles was determined by IF. As expected, on days 7 and 21, AAVP particles were localized to the tumor-associated vasculature only in mice treated with AAVP-TNF- α (Figures 4a and c). Furthermore, AAVP particles were not observed in any normal tissue vasculature (Figures 4b and d), consistent with our previously reported results.^{19,20}

AAVP-mediated TNF- α expression in tumor tissues

On days 7 and 21, the levels of TNF- α mRNA were significantly increased in tumor tissues from groups treated with targeted AAVP-TNF- α in comparison with groups lacking AAVP-TNF- α treatment ($P < 0.01$ or 0.001 ; Figures 5a-1 and a-2). We also quantified TNF- α mRNA levels in normal tissues after treatment with AAVP-TNF- α (Figures 5b-1, b-2, c-1 and c-2). Consistent with the localization of AAVP, TNF- α was not detected in normal tissues from mice receiving targeted AAVP-TNF- α .

We also measured levels of TNF- α protein in peripheral blood, tumor and normal tissues by ELISA at days 7 and 21. Consistent with the RT-PCR results, mice receiving targeted AAVP-TNF- α exhibited significantly increased expression of TNF- α in tumor tissues in comparison with those mice not receiving AAVP-TNF- α ($P < 0.001$; Figures 6a-1 and a-2), but not in peripheral blood and

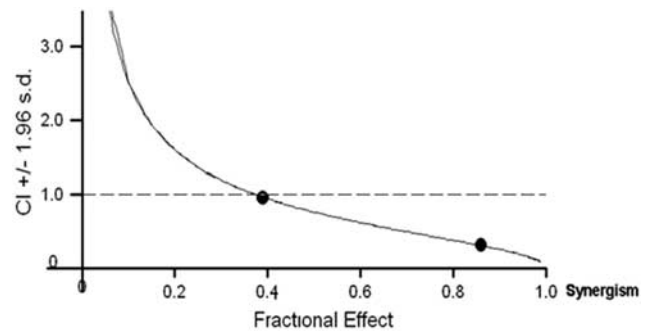


Figure 3. Synergistic effect of adeno-associated virus bacteriophage-tumor necrosis factor- α (AAVP-TNF- α) and LCL161 in M21 xenograft nude mice. The curve shows the Fraction Effect–Combination Indices plot for the combination of AAVP-TNF- α and LCL161 with the CalcuSyn Software. These results indicated that AAVP-TNF- α and LCL161 were synergistic with CI values < 1 . Fractional effect: % CK (tumor cell killing) = $(\text{Volume}_{\text{Control}} - \text{Volume}_{\text{Treat}}) / \text{Volume}_{\text{Control}}$; CI, combination index; CI < 1 : synergism is indicated.

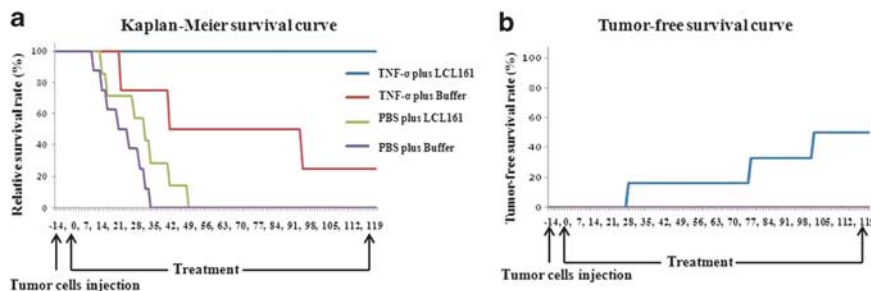


Figure 2. Survival time of mice treated with adeno-associated virus bacteriophage-tumor necrosis factor- α (AAVP-TNF- α) and LCL161. **(a)** Kaplan–Meier survival curve. The mice were treated with AAVP-TNF- α plus LCL161; AAVP-TNF- α plus sodium acetate-acetic acid (NaAc) Buffer; phosphate-buffered saline (PBS) plus LCL161; and PBS plus NaAc Buffer and monitored over time for their survival. **(b)** Tumor-free survival curve for treatment with AAVP-TNF- α plus LCL161 (blue), AAVP-TNF- α plus NaAc Buffer (red), PBS plus LCL161 (green) and PBS plus NaAc Buffer (purple). Each day represents the number of mice that were tumor free at the indicated time point.

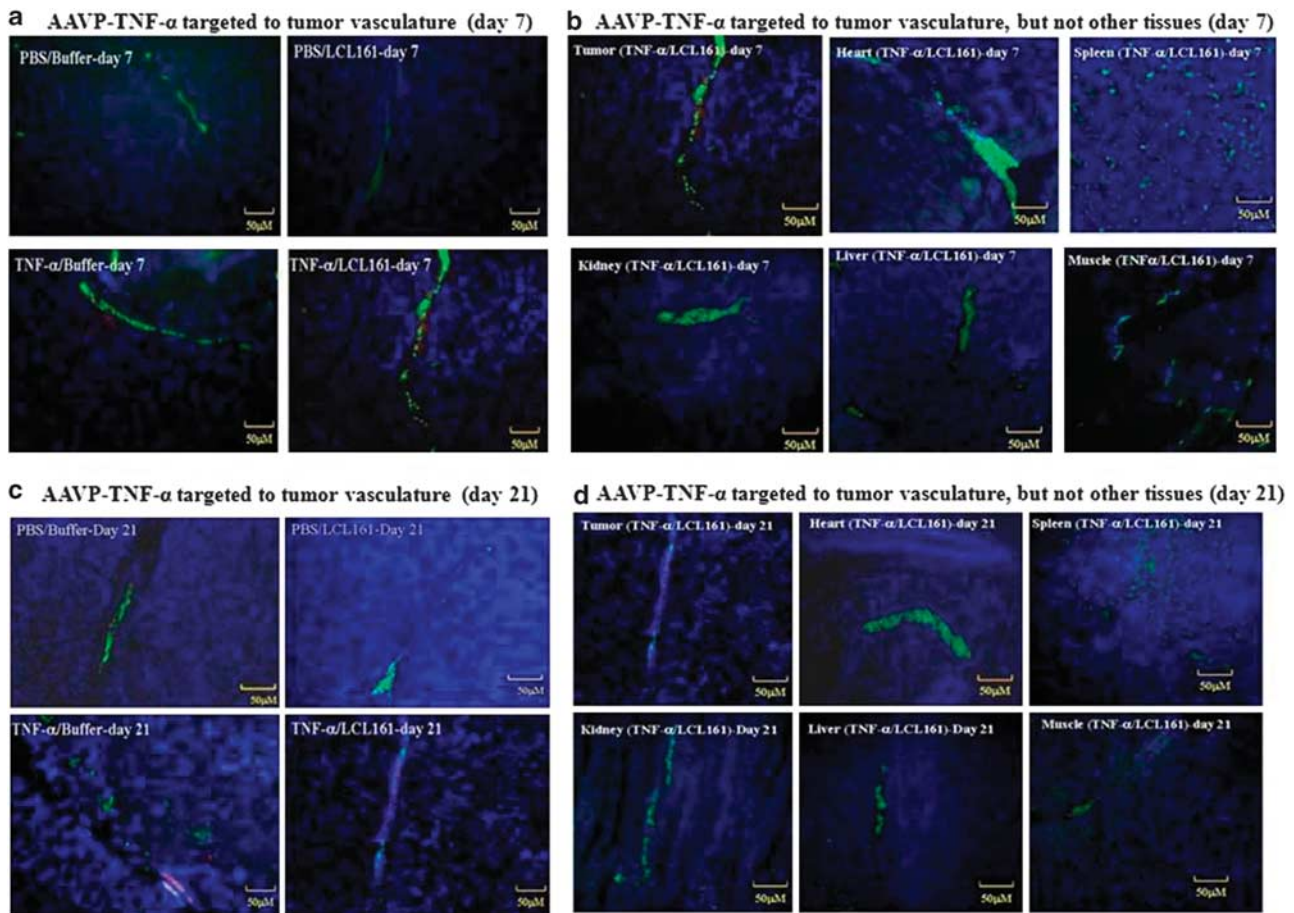


Figure 4. RGD-AAVP-TNF- α targeted specifically to tumor vasculature after systemic administration. Tumor and normal tissues (heart, spleen, kidney, liver and muscle) from all groups were analyzed for AAVP particles by immunofluorescence assay (IF). AAVP particles were stained red with anti-bacteriophage antibody (Alexa Fluor 647), tumor vasculature was stained green with CD31 antibody (Alexa Fluor 488) and nuclei were stained blue with 4,6-diamidino-2-phenylindole (DAPI). Scale bar = 50 μ m. Magnification \times 200. The adeno-associated virus bacteriophage-tumor necrosis factor- α (AAVP-TNF- α) selectively targeted tumor-associated vasculature in AAVP-TNF- α -treated groups and was absent in nontargeted AAVP-TNF- α groups by day 7 (**a**) and day 21 (**c**) after injection; AAVP-TNF- α only selectively targeted tumor-associated vasculature and was absent from normal tissues (heart, spleen, kidney, liver and muscle) in the AAVP-TNF- α -treated groups on day 7 (**b**) and day 21 (**d**) after injection.

normal tissues, confirming the tumor-selective delivery of TNF- α (Supplementary Figure S6B-1, S6B-2 and S6C).

Enhancement of tumor sensitivity to the induction of apoptosis with combined AAVP-TNF- α and LCL161

The combination of AAVP-TNF- α and LCL161 resulted in an increased proportion of apoptotic cells in the tumor tissues, \sim 41% on day 7 (Figures 7a and c) and 83% on day 21 (Figures 7b and d), compared with only 10% on day 7 (Figures 7a and c) and 20% on day 21 (Figures 7b and d) for treatment with either AAVP-TNF- α alone or LCL161 alone. Thus, the combination of AAVP-TNF- α and LCL161 induced apoptosis within tumor tissues to a greater degree than treatment with either AAVP-TNF- α or LCL161 alone ($P < 0.01$; Figures 7c and d), supporting our data for tumor response and survival (Figures 1 and 2).

LCL161 mediates the degradation of cIAP1 and cIAP2

mRNA expression of cIAP1 and cIAP2 were examined in all four groups. In mice receiving LCL161, cIAP1 and cIAP2 mRNA expression levels were significantly decreased as compared with the mice without LCL161 treatment on days 7 and 21 ($P < 0.01$;

Figure 8). These results indicated that LCL161 can mediate the degradation of cIAP1 and cIAP2 and induce apoptosis.

Activation of apoptotic pathways in response to expression of caspase 3 and caspase 9 after therapy with a combination of AAVP-TNF- α and LCL161

To characterize further the activation of apoptotic pathways as a result of treatment with AAVP-TNF- α and LCL161, we performed a series of IF experiments using antibodies that recognize caspase 3 and caspase 9. Only the active forms of caspase 3 and caspase 9 are recognized by these antibodies. Tumors treated with the combination of targeted AAVP-TNF- α and LCL161 exhibited the highest levels of active caspase 3, relative to either AAVP-TNF- α alone or LCL161 alone, as well as controls on day 7 (Figures 9a and c) and day 21 (Figures 9b and d).

The high-affinity binding of LCL161 to XIAP results in the destruction of cIAP1 and cIAP2, a reaction that precipitates the activation of noncanonical nuclear factor- κ B signaling and subsequent increased TNF- α production and further induction of caspase 9.²⁶⁻²⁹ We observed that the levels of active caspase 9 in the tumors increased significantly after treatment with the combination of targeted AAVP-TNF- α and LCL161, relative to

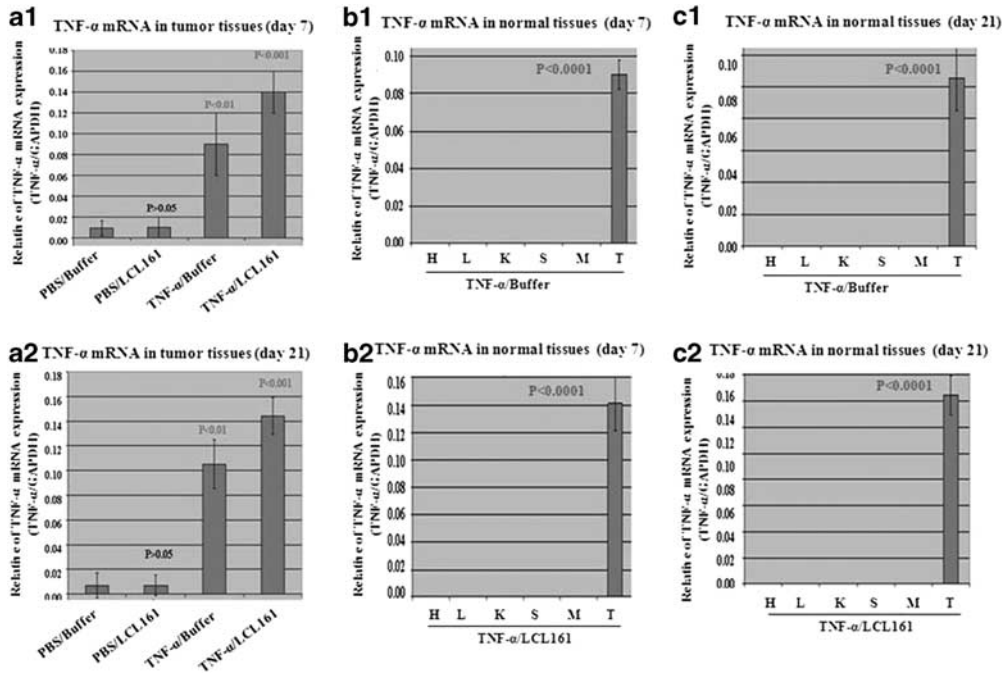


Figure 5. RGD-AAVP-TNF- α trafficking resulted in selective expression of human TNF- α mRNA in tumor tissue. Levels of human TNF- α mRNA from tumor and normal tissues (heart, spleen, kidney, liver and muscle) from all groups were analyzed by TaqMan assay. The Y axis represents the relative human TNF- α mRNA levels after normalization to glyceraldehyde-3-phosphate dehydrogenase (GAPDH) mRNA. All data are shown as mean \pm s.d. (**a1**, **a2**) mRNA levels of human TNF- α in tumor tissues were significantly increased in targeted AAVP-TNF- α -treated groups in comparison with the other groups on days 7 and 21 after injection ($P < 0.01$ or $P < 0.001$, respectively). (**b1**, **b2**, **c1**, **c2**) mRNA levels of human TNF- α were detected only in tumors and absent in normal tissues from targeted AAVP-TNF- α -treated groups (AAVP-TNF- α alone and AAVP-TNF- α plus LCL161) on day 7 ($P < 0.0001$) (**b1**, **b2**) and day 21 after injection ($P < 0.0001$) (**c1**, **c2**). H, heart; K, kidney; L, liver; M, muscle; S, spleen; T, tumor.

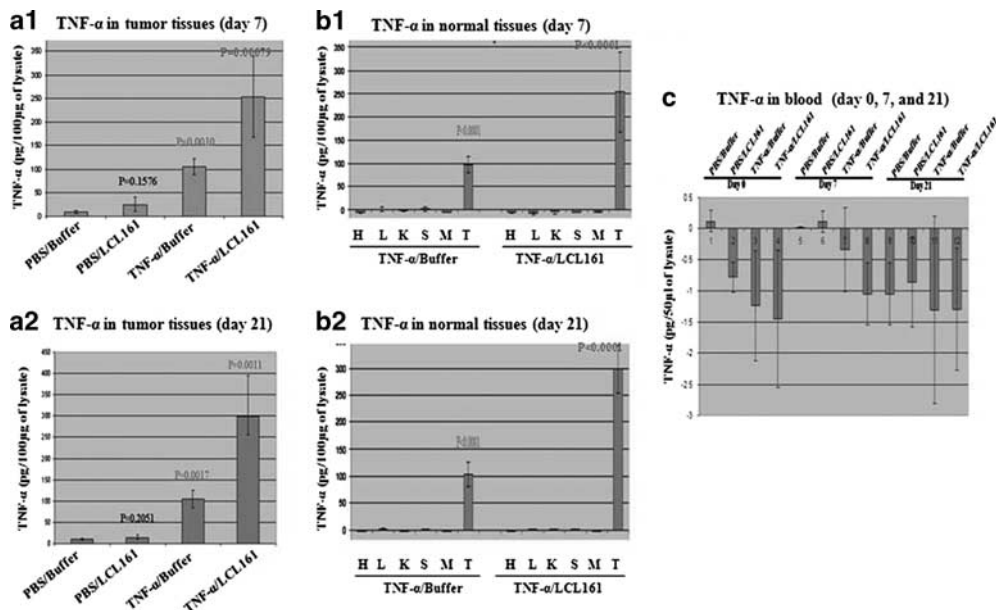


Figure 6. RGD-AAVP-TNF- α trafficking resulted in selective human TNF- α expression in tumor tissue. The levels of human TNF- α protein from tumor, normal tissues (heart, spleen, kidney, liver and muscle) and peripheral blood of all groups were evaluated by enzyme-linked immunosorbent assay (ELISA). The Y axis represents human TNF- α in 100 μ g of lysate or 50 μ l of peripheral blood. All data are shown as mean \pm s.d. (**a1**, **a2**) The level of human TNF- α in tumor tissues was significantly increased in targeted AAVP-TNF- α -treated groups compared with other groups on days 7 and 21 after injection ($P < 0.001$). (**b1**, **b2**) The expression of human TNF- α was detected only in tumors and absent in normal tissues from targeted AAVP-TNF- α -treated groups (AAVP-TNF- α alone and AAVP-TNF- α plus LCL161) on days 7 and 21 after injection ($P < 0.0001$). (**c**) Human TNF- α was absent in peripheral blood from all four groups at pretreatment (day 0) and on days 7 and 21 after treatment with targeted AAVP-TNF- α injected systemically.

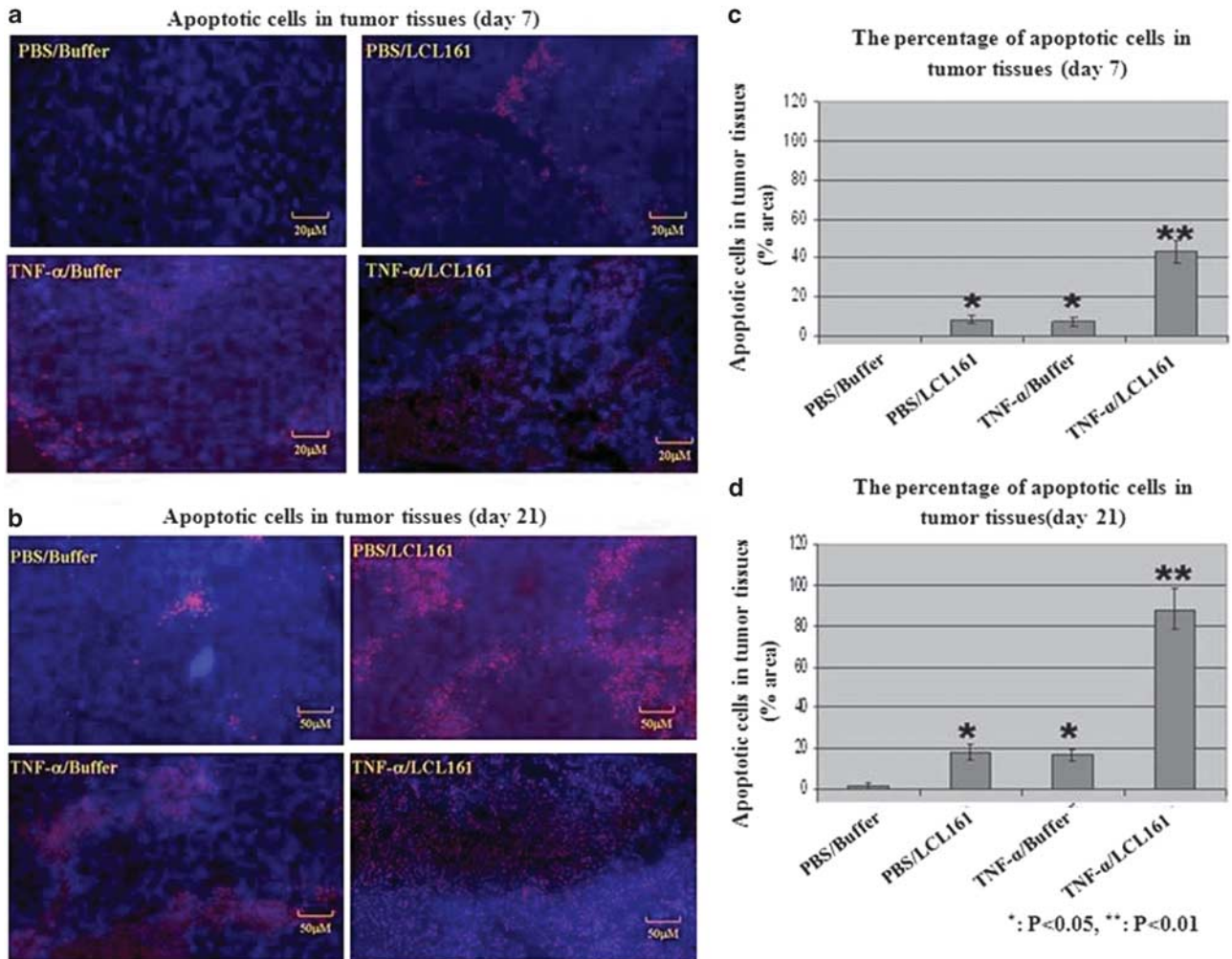


Figure 7. Apoptosis was induced and enhanced in tumor and tumor vasculature by the combination of adeno-associated virus bacteriophage-tumor necrosis factor- α (AAVP-TNF- α) and LCL161. Apoptotic cell nuclei in tumor tissues from all groups were detected on days 7 and 21 after treatment. Apoptotic cells were stained red by TUNEL (terminal deoxynucleotidyltransferase-mediated dUTP nick end labeling) assay and nuclei were stained blue with 4,6-diamidino-2-phenylindole (DAPI). Scale bar = 20 μm and 50 μm . The apoptotic index was defined as the average number of apoptotic cells per high power view counted from six sections from three mice at each time point. All data are shown as mean \pm s.d. The number of apoptotic cells in tumor tissues was increased in treated groups compared with the control group on day 7 (**a**) and day 21 (**b**) after treatment. The combination of targeted AAVP-TNF- α plus LCL161 exhibited the greatest number of apoptotic cells compared with either AAVP-TNF- α alone or LCL161 alone (magnification $\times 200$). (**c**, **d**) The number of apoptotic cells in the tumor tissues was quantified by apoptotic index. The apoptotic index in tumor tissues was increased significantly in the treatment groups compared with the control group on days 7 and 21 after treatment ($P < 0.05$). The combination of AAVP-TNF- α and LCL161 resulted in the highest apoptotic index in comparison with either AAVP-TNF- α alone or LCL161 alone on days 7 and 21 after treatment ($P < 0.001$). * $P < 0.05$; ** $P < 0.01$.

either AAVP-TNF- α alone or LCL161 alone or to control groups on day 7 (Figures 10a and c) and day 21 (Figures 10b and d). Thus, the combination of AAVP-TNF- α and LCL161 enhance tumor-specific apoptosis through the activation of pathways in which caspase 3 and 9 participate.

Effect of the combination of targeted AAVP-TNF- α plus LCL161 on cell proliferation

To identify alternative mechanisms causing the antitumor effect seen with the combination of targeted AAVP-TNF- α and LCL161, we also examined cell proliferation by IF with anti-PCNA antibody. We found no differences in cell proliferation in any of the treated groups compared with controls and no evidence of inhibition of cell proliferation ($P > 0.05$; Supplementary Figure S2A–D). This observation further supports an apoptotic mechanism rather than

an inhibition of proliferation as an explanation for the effects on tumor growth that we observed.

DISCUSSION

In this study we used a tumor vasculature-targeted hybrid vector for sustained expression of TNF- α along with chemotherapeutic agent, LCL161, and tested whether the combination could enhance tumor growth inhibition and augment the pro-apoptotic activity of TNF- α . Recently, it was reported that breast cancer cell growth was inhibited by the combination of TNF- α and LCL161.³⁵ Our results further show that the combination therapy was synergistic and resulted in enhanced tumor regression as well as prolonged tumor-free survival compared with either drug alone. We observed significant levels of TNF- α protein in tumor tissues on day 7 after intravenous injection of AAVP-TNF- α . The observed

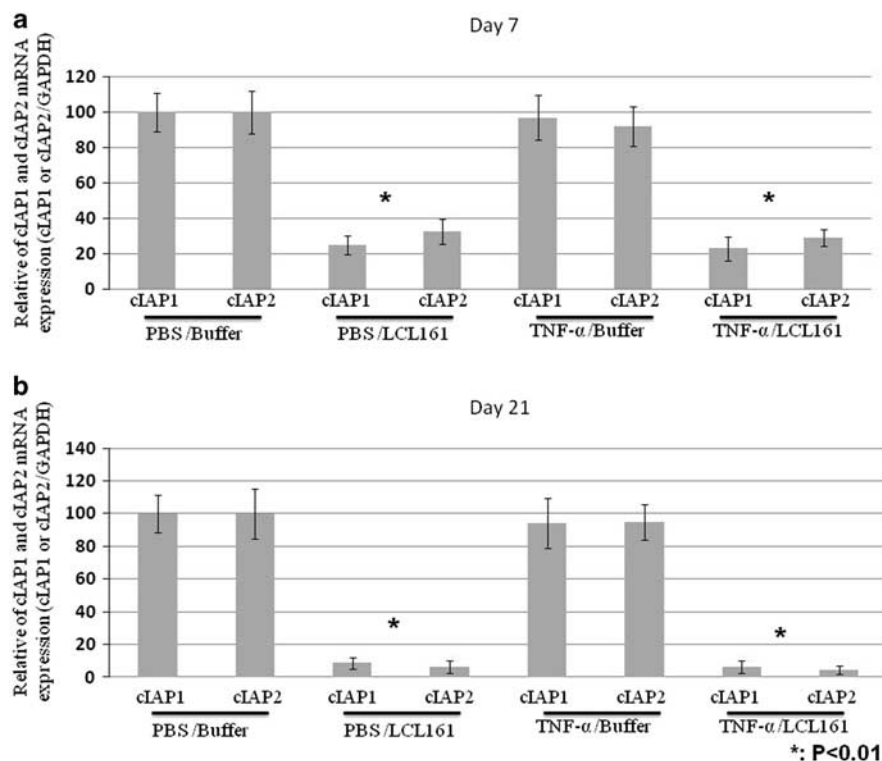


Figure 8. mRNA expression levels of cellular inhibitor of apoptosis 1 and 2 (cIAP1 and cIAP2) were significantly decreased by LCL161 treatment. mRNA levels of cIAP1 and cIAP2 from tumor tissues in all groups were analyzed by real-time reverse-transcriptase-PCR (RT-PCR) assay. The Y axis represents the relative cIAP1 and cIAP2 mRNA levels after normalization to glyceraldehyde-3-phosphate dehydrogenase (GAPDH) mRNA. All data are shown as mean \pm s.d. mRNA levels of cIAP1 and cIAP2 in tumor tissues were significantly decreased in receiving LCL161-treated groups in comparison without LCL161-treated groups on day 7 (a) and day 21 (b) after injection (* P < 0.01).

synergism with LCL161 is because of the fact that TNF- α increases the vascular permeability leading to improved penetration of LCL161 within the tumor tissues.^{36,37} Additionally, LCL161 inhibits IAPs, not only facilitating the apoptotic activity of TNF- α but also increasing the production of TNF- α by the activation of noncanonical nuclear factor- κ B signaling.^{26–30} This would account for the increased levels of TNF- α seen in the combination group than in the TNF- α -alone group. Also reported was that LBW 242, a Smac mimetic, induces degradation of cIAPs and TNF- α expression.³⁸ Furthermore, by inhibiting XIAP, cIAP1 and cIAP2, LCL161 prevents the development of resistance to apoptotic pathways induced by TNF- α .^{31,32} This would explain the observed resistance and relapse thereafter seen in the TNF- α -alone therapy group during the second cycle of treatment. This did not occur in the combination group. As many cancer cells inhibit the natural TNF- α -mediated cell death machinery of apoptosis by activating the IAPs, Smac inhibitor LCL161 is the ideal agent to combine with our novel tumor-targeted TNF- α therapy. One of the drawbacks of using TNF- α or LCL161 alone was that the apoptotic effects of either agents on the tumor tissues was not complete with no tumor-free survival. The combination therapy increased the overall tumor-free survival rate to 50%, thereby suggesting that the combination therapy not only leads to complete regression of tumor but also prevents recurrence. We observed 100% survival in the combination group compared with 25% in either group alone, therefore suggesting a survival advantage with lower toxicity in the combination therapy. It is important to note that as all the mice in the combination group (except one mouse that died because of a skin condition unrelated to the tumor) were alive at the end of the

90-day period, further treatment could hypothetically achieve 100% tumor-free survival.

TNF- α demonstrates species preference for toxicity; therefore, the evaluation of human TNF- α in a mouse model can underestimate the potential toxicities.^{39–41} However, in the current study, we confirmed the tumor-selective trafficking of AAVP particles and the absence of detectable TNF- α in any control tissue. We also demonstrated the absence of systemic toxicity to both AAVP-TNF- α and LCL161 in all of the four groups of mice. Furthermore, as the Smac mimetics are not targeted whereas the TNF- α vectors are, this combination is likely to be better tolerated than current cancer therapies. The synergistic effect of the combination therapy will also allow for lower doses to be used, which will further reduce the side effects.

We learnt that the combination therapy predominantly acts by inducing apoptosis and has no effect on proliferation. This was confirmed by demonstrating elevated levels of caspase 3 and caspase 9. Caspase 9 is an initiator caspase that cleaves inactive pro-forms of effector caspases, thereby activating the effector caspases. Caspase 3 is an effector caspase that, in turn, cleaves other protein substrates within the cell to activate the apoptotic process. Their levels were increased to a greater extent in the combination group than in the TNF- α - and LCL161-alone groups, thereby confirming that the combination group has synergistic apoptotic effects. TNF- α induces the apoptosis of tumor tissues including the tumor vascular endothelial cells, and thereby it can potentially decrease vascular metastasis of tumor by disrupting the tumor vasculature. To our knowledge, we are the first to pioneer targeted gene therapy with chemotherapy. Tumor-targeted p53 gene therapy enhancing the efficacy of conventional

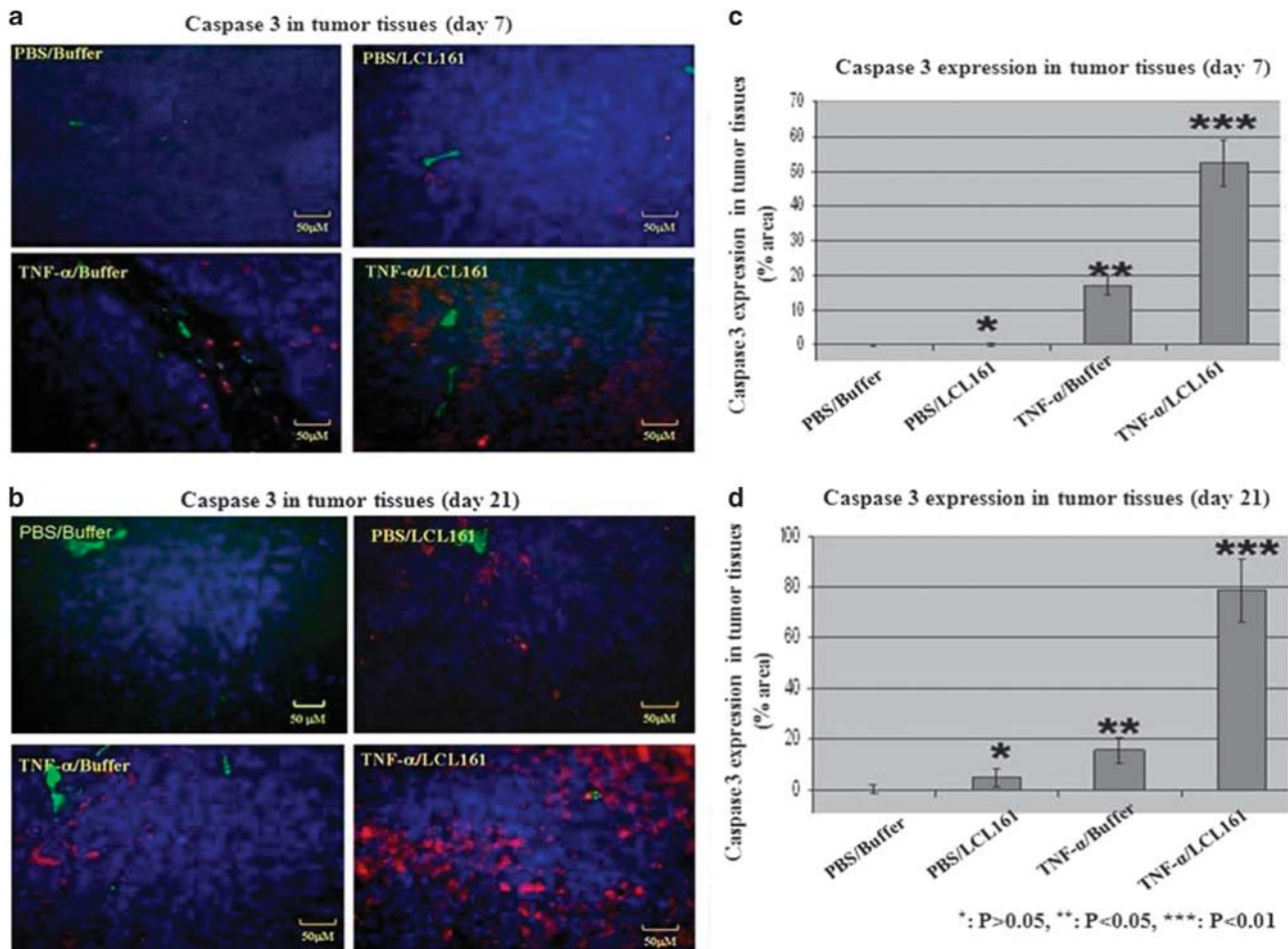


Figure 9. The combination of adeno-associated virus bacteriophage-tumor necrosis factor- α (AAVP-TNF- α) and LCL161 increases the expression of active caspase 3 in tumor tissues. The active caspase 3 was analyzed in tumor sections from the treatment groups on days 7 and 21 after treatment by immunofluorescence assay (IF). Active caspase 3 was stained red by an anti-caspase 3 antibody (Alexa Fluor 647), blood vessels were stained green by an anti-CD31 antibody (Alexa Fluor 488) and nuclei were stained blue with 4,6-diamidino-2-phenylindole (DAPI). Scale bar = 50 μ m. **(a)** The expression of active caspase 3 in tumor tissues was increased in the treatment groups compared with the control group on day 7 after treatment. The expression of active caspase 3 was the highest in the group receiving the combination of targeted AAVP-TNF- α plus LCL161 in comparison with either AAVP-TNF- α alone or LCL161 alone (magnification \times 200). **(b)** The expression of active caspase 3 in tumor tissues was increased in the treated groups compared with the control group on day 21 after treatment. The combination of AAVP-TNF- α and LCL161 resulted in the highest level of caspase 3, relative to that seen in tissues treated with either AAVP-TNF- α alone or LCL161 alone (magnification \times 200). **(c, d)** The expression of active caspase 3 in tumor tissues was quantified and was increased significantly in the treated groups compared with the control group on day 7 **(c)** and day 21 **(d)** after treatment ($P < 0.05$ or $P < 0.001$, respectively). The levels of active caspase 3 was the highest in the group receiving the combination of targeted AAVP-TNF- α and LCL161 in comparison with groups treated with either AAVP-TNF- α alone or LCL161 alone on day 7 **(c)** and day 21 **(d)** after treatment ($P < 0.001$). * $P > 0.05$; ** $P < 0.05$; *** $P < 0.01$.

chemotherapy or radiotherapy has been reported.⁴² A recent phase 2 trial using TNF- α and chemotherapy has shown that TNF- α can enhance the effectiveness of chemotherapy significantly.⁴³ The single-agent activity of Smac mimetics is limited and combinations of Smac mimetics with TRAIL (TNF-related apoptosis-inducing ligand) have also been reported to have therapeutic potential for cancer treatment.⁴⁴ Furthermore, degradation of IAPs by Smac mimetics results in enhancing TNF- α -induced apoptosis, as in the absence of the IAP complexes detaching from the TNF receptor 1 favoring the formation of a RIP1-dependent caspase 8 activating complex.^{45,46} Our studies demonstrated the synergistic effect of the combination therapy of TNF- α and IAPs inhibitor. Furthermore, our technique of delivering TNF- α directly to the tumor vasculature will eliminate the systemic side effects of TNF- α , and the addition of IAP inhibitors will

improve the efficacy and prevent the development of resistance to TNF- α .

In summary, our results demonstrate that the combination of targeted gene therapy with AAVP-TNF- α and oral administration of the Smac mimetic, LCL161, has synergistic antitumor activity. This activity results from the induction of apoptosis in the tumor cells and the tumor-associated vasculature. Survival was prolonged significantly in all animals treated with the combination. We conclude that combinatorial therapy with targeted AAVP-TNF- α and LCL161 can enhance efficacy, and reduce toxicity, as well as prevent and/or delay the development of resistance. We believe that this novel strategy of targeted gene therapy with AAVP-TNF- α and targeting IAPs with LCL161 will be of benefit to patients with cancer. Further studies will advance this novel approach to the clinic.

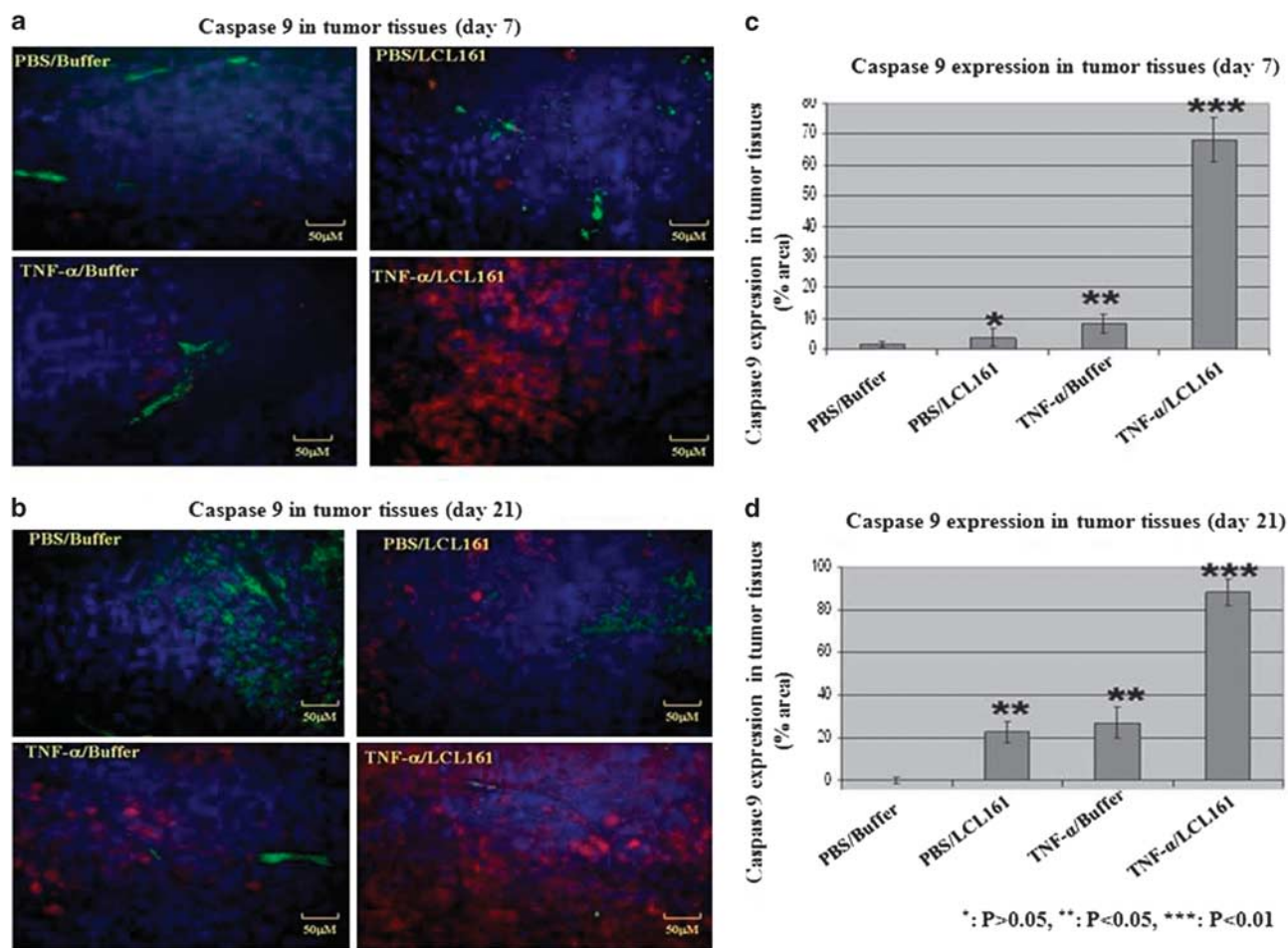


Figure 10. The combination of adeno-associated virus bacteriophage-tumor necrosis factor- α (AAVP-TNF- α) and LCL161 increased the expression of active caspase 9 in tumor tissues. Expression of active caspase 9 was analyzed by immunofluorescence assay (IF) in tumor sections from the treated and control groups on days 7 and 21 after treatment. Active caspase 9 was stained red by an anti-caspase 9 antibody (Alexa Fluor 647), blood vessels were stained green by an anti-CD31 antibody (Alexa Fluor 488) and nuclei were stained blue with 4,6-diamidino-2-phenylindole (DAPI). Scale bar = 50 μ m. **(a)** Levels of active caspase 9 in tumor tissues were increased in treated groups compared with the control on day 7 after treatment. The highest expression of active caspase 9 in tumor tissues was seen in the group receiving combination targeted AAVP-TNF- α plus LCL161 in comparison either AAVP-TNF- α alone or LCL161 alone (magnification $\times 100$). **(b)** The expression of active caspase 9 in tumor tissues was increased in the treated groups compared with the control group on day 21 after treatment. Similarly, active caspase 9 in tumor tissues was highest in the targeted AAVP-TNF- α plus LCL161-treated group relative to groups treated with either AAVP-TNF- α alone or LCL161 alone (magnification $\times 100$). **(c, d)** Active caspase 9 in tumor tissues was quantified. Levels were increased significantly in the treated groups compared with the control group on day 7 **(c)** and day 21 **(d)** after treatment ($P < 0.05$ or $P < 0.001$, respectively). Active caspase 9 was highest after combined AAVP-TNF- α and LCL161 administration in comparison with that of either AAVP-TNF- α alone or LCL161 alone on day 7 **(c)** and day 21 **(d)** after treatment ($P < 0.001$). * $P > 0.05$; ** $P < 0.05$; *** $P < 0.01$.

CONFLICT OF INTEREST

The authors declare no conflict of interest.

ACKNOWLEDGEMENTS

We thank Novartis Pharmaceuticals and Dale Porter, Brant Firestone and Claudina Stevenson for informative discussions. This work was supported in part through a generous gift from Linda and Earl Altman.

REFERENCES

- Larocca D, Kassner PD, Witte A, Ladner RC, Pierce GF, Baird A. Gene transfer to mammalian cells using genetically targeted filamentous bacteriophage. *FASEB J* 1999; **13**: 727–734.
- Barrow PA, Soothill JS. Bacteriophage therapy and prophylaxis: rediscovery and renewed assessment of potential. *Trends Microbiol* 1997; **5**: 268–271.
- Ivanenkov V, Felici F, Menon AG. Uptake and intracellular fate of phage display vectors in mammalian cells. *Biochim Biophys Acta* 1999; **1448**: 450–462.
- Weber-Dabrowska B, Mulczyk M, Gorski A. Bacteriophages as an efficient therapy for antibiotic-resistant septicemia in man. *Transplant Proc* 2003; **35**: 1385–1386.
- Borysowski J, Gorski A. Is phage therapy acceptable in the immunocompromised host? *Int J Infect Dis* 2008; **12**: 466–471.
- Bartlett DL, Buell JF, Libutti SK, Reed E, Lee KB, Figg WD *et al*. A phase I trial of continuous hyperthermic peritoneal perfusion with tumor necrosis factor and cisplatin in the treatment of peritoneal carcinomatosis. *Cancer* 1998; **83**: 1251–1261.
- Bartlett DL, Libutti SK, Figg WD, Fraker DL, Alexander HR. Isolated hepatic perfusion for unresectable hepatic metastases from colorectal cancer. *Surgery* 2001; **129**: 176–187.
- Alexander Jr. HR, Bartlett DL, Libutti SK, Fraker DL, Moser T, Rosenberg SA. Isolated hepatic perfusion with tumor necrosis factor and melphalan for unresectable cancers confined to the liver. *J Clin Oncol* 1998; **16**: 1479–1489.
- Alexander Jr. HR, Bartlett DL, Libutti SK. Current status of isolated hepatic perfusion with or without tumor necrosis factor for the treatment of unresectable cancers confined to liver. *Oncologist* 2000; **5**: 416–424.
- Alexander HR, Libutti SK, Bartlett DL, Puhlmann M, Fraker DL, Bachheimer LC. A phase I-II study of isolated hepatic perfusion using melphalan with or without

- tumor necrosis factor for patients with ocular melanoma metastatic to liver. *Clin Cancer Res* 2000; **6**: 3062–3070.
- 11 Alexander Jr. HR, Libutti SK, Bartlett DL, Pingpank JF, Kranda K, Helsabeck C *et al*. Hepatic vascular isolation and perfusion for patients with progressive unresectable liver metastases from colorectal carcinoma refractory to previous systemic and regional chemotherapy. *Cancer* 2002; **95**: 730–736.
 - 12 Libutti SK, Barlett DL, Fraker DL, Alexander HR. Technique and results of hyperthermic isolated hepatic perfusion with tumor necrosis factor and melphalan for the treatment of unresectable hepatic malignancies. *J Am Coll Surg* 2000; **191**: 519–530.
 - 13 Lans TE, Bartlett DL, Libutti SK, Gnatt MF, Liewehr DJ, Venzon DJ *et al*. Role of tumor necrosis factor on toxicity and cytokine production after isolated hepatic perfusion. *Clin Cancer Res* 2001; **7**: 784–790.
 - 14 Lejeune FJ, Lienard D, Matter M, Ruegg C. Efficiency of recombinant human TNF in human cancer therapy. *Cancer Immunol* 2006; **6**: 6.
 - 15 Rivera F, Lopez-Tarruella S, Vega-Villegas ME, Salcedo M. Treatment of advanced pancreatic cancer: from gemcitabine single agent to combinations and targeted therapy. *Cancer Treat Rev* 2009; **35**: 335–339.
 - 16 Hajitou A, Trepel M, Lilley CE, Soghomonyan S, Alauddin MM, Marini 3rd FC *et al*. A hybrid vector for ligand-directed tumor targeting and molecular imaging. *Cell* 2006; **125**: 385–398.
 - 17 Hajitou A, Rangel R, Trepel M, Soghomonyan S, Gelovani JG, Alauddin MM *et al*. Design and construction of targeted AAVP vectors for mammalian cell transduction. *Nat Protoc* 2007; **2**: 523–531.
 - 18 Pasqualini R, Koivunen E, Ruoslahti E. A peptide isolated from phage display libraries is a structural and functional mimic of an RGD-binding site on integrins. *J Cell Biol* 1995; **130**: 1189–1196.
 - 19 Tandle A, Hanna E, Lorang D, Hajitou A, Moya CA, Pasqualini R *et al*. Tumor vasculature-targeted delivery of tumor necrosis factor- α . *Cancer* 2009; **115**: 128–139.
 - 20 Paoloni MC, Tandle A, Mazcko C, Hanna E, Kachala S, Leblanc A *et al*. Launching a novel preclinical infrastructure: comparative oncology trials consortium directed therapeutic targeting of TNF α to cancer vasculature. *PLoS One* 2009; **4**: e4972.
 - 21 Gyrd-Hansen M, Meier P. IAPs: from caspase inhibitors to modulators of NF- κ B, inflammation and cancer. *Nat Rev Cancer* 2010; **10**: 561–574.
 - 22 Gray D, McKenzie MD, Nachbur U, Huang DC, Bouillet P, Thomas HE *et al*. XIAP discriminates between type I and type II FAS-induced apoptosis. *Nature* 2009; **460**: 1035–1039.
 - 23 Wu G, Chai J, Suber TL, Wu JW, Du C, Wang X *et al*. Structural basis of IAP recognition by Smac/DIABLO. *Nature* 2000; **408**: 1008–1012.
 - 24 Srinivasula SM, Hegde R, Saleh A, Datta P, Shiozaki E, Chai J *et al*. A conserved XIAP-interaction motif in caspase-9 and Smac/DIABLO regulates caspase activity and apoptosis. *Nature* 2001; **410**: 112–116.
 - 25 Chen KF, Lin JP, Shiau CW, Tai WT, Liu CY, Yu HC *et al*. Inhibition of Bcl-2 improves effect of LCL161, a SMAC mimetic, in hepatocellular carcinoma cells. *Biochem Pharmacol* 2012; **84**: 268–277.
 - 26 Kurbanov BM, Fecker LF, Geilen CC, Sterry W, Eberle J. Resistance of melanoma cells to TRAIL does not result from upregulation of antiapoptotic proteins by NF- κ B but is related to downregulation of initiator caspases and DR4. *Oncogene* 2007; **26**: 3364–3377.
 - 27 Gaither A, Porter D, Yao Y, Borawski J, Yang G, Donovan J *et al*. A Smac mimetic rescue screen reveals roles for inhibitor of apoptosis proteins in tumor necrosis factor- α signaling. *Cancer Res* 2007; **67**: 11493–11498.
 - 28 Varfolomeev E, Goncharov T, Fedorova AV, Dynek JN, Zobel K, Deshayes K *et al*. c-IAP1 and c-IAP2 are critical mediators of tumor necrosis factor alpha (TNF α)-induced NF- κ B activation. *J Biol Chem* 2008; **283**: 24295–24299.
 - 29 Mahoney DJ, Cheung HH, Mirad RL, Plenchette S, Simard C, Enwere E *et al*. Both cIAP1 and cIAP2 regulate TNF α -mediated NF- κ B activation. *Proc Natl Acad Sci USA* 2008; **105**: 11778–11783.
 - 30 Bertrand MJ, Milutinovic S, Dickson KM, Ho WC, Boudreault A, Durkin J *et al*. cIAP1 and cIAP2 facilitate cancer cell survival by functioning as E3 ligases that promote RIP1 ubiquitination. *Mol Cell* 2008; **30**: 689–700.
 - 31 Ashkenazi A, Herbst RS. To kill a tumor cell: the potential of proapoptotic receptor agonists. *J Clin Invest* 2008; **118**: 1979–1990.
 - 32 Newsom-Davis T, Prieske S, Walczak H. Is TRAIL the holy grail of cancer therapy? *Apoptosis* 2009; **14**: 607–623.
 - 33 Damaraju VL, Bouffard DY, Wong CK, Clarke ML, Mackey JR, Leblond L *et al*. Synergistic activity of troxacitabine (Troxytyl) and gemcitabine in pancreatic cancer. *BMC Cancer* 2007; **7**: 121.
 - 34 Thoennissen NH, Iwanski GB, Doan NB, Okamoto R, Lin P, Abbassi S *et al*. Cucurbitacin B induces apoptosis by inhibition of the JAK/STAT pathway and potentiates antiproliferative effects of gemcitabine on pancreatic cancer cells. *Cancer Res* 2009; **69**: 5876–5884.
 - 35 Firestone B, Conway C, Yang G, Gao H, Porter D, Slisz J *et al*. Correlation between TNF α and LCL161 anti-tumor activity in patient derived xenograft models of human cancer. AACR-NCI-EORTC International Conference: Molecular Targets and Cancer Therapeutics—Nov 15–19; Boston, MA 2009.
 - 36 Friedl J, Puhlmann M, Bartlett DL, Libutti SK, Turner EN, Gnatt MF *et al*. Induction of permeability across endothelial cell monolayers by tumor necrosis factor (TNF) occurs via a tissue factor-dependent mechanism: relationship between the pro-coagulant and permeability effects of TNF. *Blood* 2002; **100**: 1334–1339.
 - 37 Kerker S, Williams M, Blocksom JM, Wilson RF, Tyburski JG, Steffes CP. TNF- α and IL-1 β increase pericyte/endothelial cell co-culture permeability. *J Surg Res* 2006; **132**: 40–45.
 - 38 Eschenburg G, Eggert A, Schramm A, Lode HN, Hundsdoerfer P. Smac mimetic LBW242 sensitizes XIAP-overexpressing neuroblastoma cells for TNF- α -independent apoptosis. *Cancer Res* 2012; **72**: 2645–2656.
 - 39 Brouckaert PG, Everaerd B, Libert C, Takahashi N, Fiers W. Species specificity and involvement of other cytokines in endotoxin shock action of recombinant tumour necrosis factor in mice. *Agents Actions* 1989; **26**: 196–198.
 - 40 Fransen L, Ruysschaert MR, Van der Heyden J, Fiers W. Recombinant tumor necrosis factor: species specificity for a variety of human and murine transformed cell lines. *Cell Immunol* 1986; **100**: 260–267.
 - 41 Kramer SM, Aggarwal BB, Eessalu TE, McCabe SM, Ferraiolo BL, Figari IS *et al*. Characterization of the in vitro and in vivo species preference of human and murine tumor necrosis factor- α . *Cancer Res* 1988; **48**: 920–925.
 - 42 Xu L, Pirolo KF, Chang EH. Tumor-targeted P53-gene therapy enhances efficacy of conventional chemotherapy. *J Control Release* 2001; **74**: 115–128.
 - 43 Li M, Xu T, Zhang Z, Xue X, Zhang C, Qin X *et al*. A Phase II multicenter, randomized, double-blind study of a recombinant mutated human tumor necrosis factor- α in combination with chemotherapies in cancer patients. *Cancer Sci* 2012; **103**: 288–295.
 - 44 Lu J, McEachern D, Sun H, Bai L, Peng Y, Qiu S *et al*. Therapeutic potential and molecular mechanism of a novel, potent, nonpeptide, Smac mimetic SM-164 in combination with TRAIL for cancer treatment. *Mol Cancer Ther* 2011; **10**: 902–914.
 - 45 Feoktistova M, Geserick P, Kellert B, Dimitrova DP, Langlais C, Hupe M *et al*. cIAPs block Ripoptosome formation, a RIP1/caspase-8 containing intracellular cell death complex differentially regulated by cFLIP isoforms. *Mol Cell* 2011; **43**: 449–463.
 - 46 Haas TL, Emmerich CH, Gerlach B. Recruitment of the linear ubiquitin chain assembly complex stabilizes the TNF-R1 signaling complex and is required for TNF-mediated gene induction. *Mol Cell* 2009; **36**: 831–844.



This work is licensed under the Creative Commons Attribution-NonCommercial-Share Alike 3.0 Unported License. To view a copy of this license, visit <http://creativecommons.org/licenses/by-nc-sa/3.0/>

Supplementary Information accompanies the paper on Cancer Gene Therapy website (<http://www.nature.com/cgt>)